DECREASE IN PHASE DENSITY IN VERY BRIGHT BEAMS

A. L. Shabalin

UDC 537.533.31

The physical processes causing an increase in the virtual size of the emitter and a decrease in brightness in beams of charged particles from point sources (autoelectron emitters, electro-gas-dynamic (EGD) ion sources, and ion sources with field ionization) are considered. The virtual size of the emitter increases because of mutual repulsion of randomly distributed beam particles. The results of the calculations agree well with the available experimental data.

INTRODUCTION

Quasi-point ion and electron sources with a high emission current density, in which charged particles are produced by processes in strong electric fields – electron field emission, ion field evaporation, and field ionization – have undergone intensive improvement in recent years. These sources are distinguished by extremely high initial brightness

$$B = j_0 W/\pi T_0 \qquad (1)$$

(j_0 is the emission current density, W is the particle energy, and T_0 is the particle temperature at the emitter surface), which has the meaning of the current emitted from a unit area into a unit solid angle.

We choose the axis along which the beam of charged particles propagates and construct a phase space of transverse coordinates and transverse momenta. In this four-dimensional space each particle will be depicted by a point, and the volume occupied by the cloud of such points is called the beam emittance, while the brightness B is proportional to the density of points in the cloud. According to the Liouville theorem, in the absence of time-dependent fields, the phase volume and brightness are the same in any beam cross section. Unfortunately, it turns out in practice that during the acceleration and transport of beams the phase volume, as a rule, undergoes a more or less pronounced increase, while the brightness decreases (exceptions are electron and positron beams in accumulators, which are strongly cooled by synchrotron emission, which leads to an increase in their brightness, as follows from (1), as well as proton and antiproton beams with electronic and stochastic cooling [1, 2]). Let us consider the possible causes of an increase in phase volume. In Fig. 1a we show a typical phase portrait of a beam from an ion source, and in Fig. 1b a portrait of the same beam that has passed through an optical system with spherical aberration. Although the actual phase volume of the beam did not change in this case, its phase portrait became complicated and the effective phase volume occupied by the beam (shown by dashed lines) increased severalfold. The average brightness decreased accordingly. This case is obviously consistent with the Liouville theorem, since the actual phase volume of the beam was conserved. But if the central part of the beam is singled out (blackened in the figure), then not only the actual but also the effective phase volume of this part of the beam remains the same.

A different situation occurs if there is mutual scattering of beam particles or oscillations develop in the beam, in which case the conditions of the Liouville theorem also cease to be satisfied (time-dependent forces develop). In the process of transport, the phase volume of the beam begins to inflate, without its shape changing significantly (Fig. 1c). If the central part of the beam is again singled out, then its phase volume also increases.

Thus, in the first case the emittance increases because of the poor quality of the ion-optical system; it is not fundamental, since one can, in principle, construct an ion-optical system that will simplify the emittance, converting the beam in Fig. 1b back into the beam in Fig. 1a, with the brightness increasing to the initial value. In the second case, on the contrary, the increase in emittance determined by the properties of the beam itself

Novosibirsk. Translated from Prikladnaya Mekhanika i Tekhnicheskaya Fizika, No. 2, pp. 3-12, March-April, 1992. Original article submitted June 20, 1991.

0021-8944/92/3302-0141$12.50

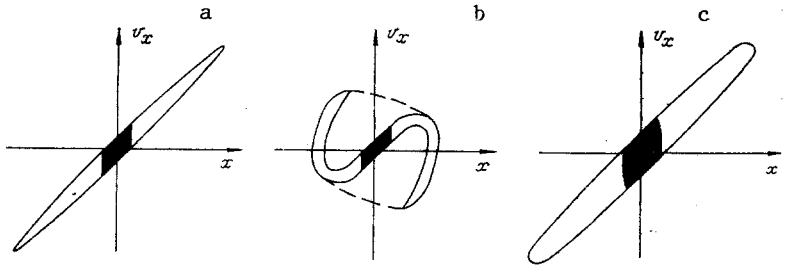

Fig. 1

will be fundamental, and the beam brightness in Fig. 1c cannot be increased by nondissipative means.

As a result of the advent of very bright quasi-point sources, a number of effects have been discovered that are typical of bright beams and lead to a fundamental decrease in their brightness. Let us consider an EGD ion emitter as an example. The typical radius of its emission zone is $r_0 \sim 2 \cdot 10^{-7}$ cm [3] and the ion temperature at the emitter surface is $T_0 \sim$ 1 eV. The ion beam from an EGD emitter expands rapidly. If we assume that the beam emittance does not increase, then at a distance r = 20 cm from the emitter the transverse ion temperature should decrease to $T_{i\perp} = T_0(r_0/r)^2$ ($T_{i\perp} \sim 10^{-16}$ eV) due to expansion of the beam. It is obvious that the slightest heating of such a cold beam, due to Coulomb repulsion of the randomly distributed ions, for example, will lead to a sharp increase in emittance.

This effect, of which it is convenient to interpret as an increase in the virtual size of the source, has been calculated numerically by the Monte-Carlo method in electron and ion beams in [4] and [5], respectively, although it is difficult to identify any relationships in the results. An attempt to calculate analytically the increase in virtual size (erroneous, in our opinion) was undertaken in [6]. Effects of Coulomb repulsion of charged particles have also been considered in [7]. In the present paper we calculate the increase in the virtual size of the source due to Coulomb repulsion of randomly distributed, charged particles in a beam and compare it with experimental results. We are concerned with ion beams below, but all of the arguments can be applied with equal success to electron beams.

THEORY

Let us define the virtual size of an emitter. Let the point A (Fig. 2) lie at a large distance r from the emitter: $r \gg a_s$ (a_s is the physical size of the emitter; a crossover beam can also be treated as an emitter). Ions arriving at this point have an angular spread $\theta \ll 1$ and the virtual size of the source is $a = \theta r = r\Delta v_\perp / v$ ($\Delta v_\perp$ is the maximum spread of transverse velocities and v is the total ion velocity).

If the beam contains no electric fields, then the virtual size of the source does not change during free dispersal of the ions (a = const) and $\Delta v_\perp$ decreases with increasing r. We now allow for the intrinsic transverse field of the beam, which can be divided arbitrarily into two components: the first is determined by the total space charge of the beam (assuming the charge to be uniformly "smeared out") and causes orderly expansion of the beam without increasing the emittance (to compensate for this expansion it is sufficient to slightly increase the focusing action of the lens); the second is determined by the discreteness of the charge of the ions and fluctuates with time, leading to an increase in emittance.

Designating the transverse fluctuation field as $F_\perp$, we write the variation of virtual size,

$$da = \frac{r}{v} dv_{\perp F}, \tag{2}$$

where $dv_{\perp F}$ is the change in transverse velocity caused by the fluctuation field,

$$dv_{\perp F} = \frac{e}{m} F_\perp \frac{dr}{v}, \tag{3}$$

and e and m are the ion charge and mass (the change in longitudinal velocity caused by the fluctuation field $F_\parallel$ leads to an increase in the energy spread of the ions [6, 8]).

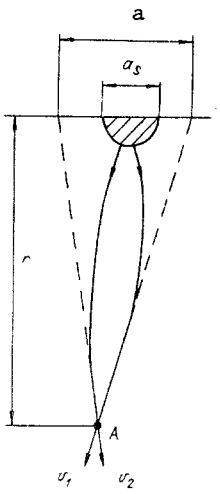

Fig. 2

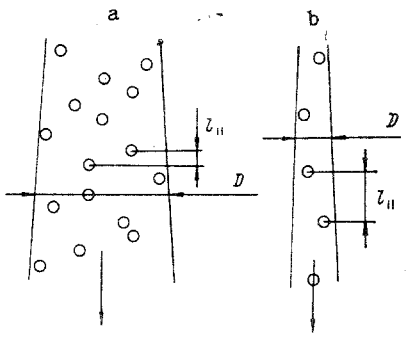

Fig. 3

Since the ion energy is $mv^2/2 = eU$ (U is the accelerating voltage), from (2) and (3) we have

$$da = \frac{F_\perp}{2U} r\, dr. \tag{4}$$

To calculate $F_\perp$ we consider two different cases (Fig. 3a and b). In the beam in Fig. 3a the average longitudinal distance between ions, $\ell_\parallel = ev/J$ (J is the ion current), is considerably less than the transverse side of the beam and each ion moves in the environment of the cloud of other ions. We call this case the "charged cloud" mode. In the beam in Fig. 3b, on the contrary,

$$l_\parallel \gg D \tag{5}$$

(D is the beam diameter), and the ions move individually, one after another, in the so-called "individual" mode. The values of $F_\perp$ in these two cases will obviously differ considerably.

To calculate $F_\perp$ in the charged cloud mode, we use the results of [9], in which the probability distribution function $p(|F|)$ has been given for the modulus of the gravitational field in a cloud of randomly distributed stars of density n. Since the electrical forces also vary as r^{-2}, the results of [9] also apply to a cloud of charged particles:

$$p(|F_\perp|) = H(\beta)/F^*,\ F^* = 2\pi(4/15)^{2/3} e n^{2/3},\ \beta = |F|/F^*,$$

$$H(\beta) = \frac{2}{\pi\beta}\int_0^\infty \exp\left[-\left(\frac{x}{\beta}\right)^{3/2}\right] x \sin x\, dx.$$

For the probability distribution function of the field component $F_\perp$, simple calculations yield

$$H(\beta_\perp) = \frac{1}{2}\int_{\beta_\perp}^\infty \frac{H(\beta)}{\beta}\, d\beta \quad (\beta_\perp = F_\perp/F^*).$$

The function $H(\beta_\perp)$ was calculated numerically, and its graph is given in Fig. 4.

In a focused beam the brightness decreases smoothly from the center toward the edges, with the current density profile basically coinciding with the function $H(\beta_\perp)$ (Fig. 4). For the emitter size we take the diameter at which the current density falls to half of that at the center. Since the width of the function $H(\beta_\perp)$ at half-height is about 3, from (4) we have

$$da = \frac{3F^*}{2U} r\, dr. \tag{6}$$

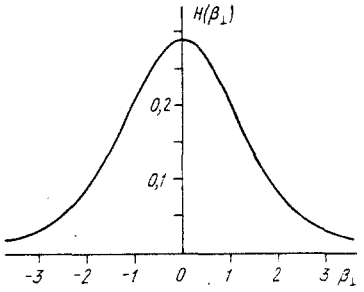

Fig. 4

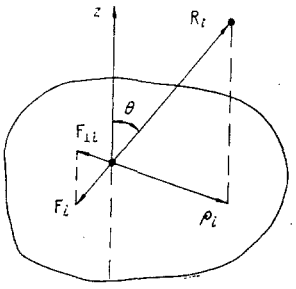

Fig. 5

For free expansion of a beam with an angular intensity I from a point source, Eq. (6) can be rewritten as

$$da = 3\pi \left(\frac{4}{15}\right)^{2/3} \left(\frac{mI^2}{2U^4}\right)^{1/3} \frac{dr}{r^{1/3}} \tag{7}$$

or

$$a_0 = \frac{9\pi}{15^{2/3}} \left(\frac{mI^2}{U^4}\right)^{1/3} \left(r_2^{2/3} - r_1^{2/3}\right) \tag{8}$$

(r_1 and r_2 are the distances from the source between which the increase in virtual size occurs).

In integrating Eq. (7) we understand that the density of ions in the beam decreases smoothly as it moves, while their relative positions do not change, i.e., mixing of the ions does not occur. If the ions do mix, then the force acting on some ion varies randomly in magnitude and direction, and Eq. (8) becomes incorrect. Let us consider the main factors that can lead to mixing of the ions.

First, an ion acquires a velocity under the action of the fluctuation field F and starts to move relative to the other ions, i.e., the potential energy of interaction of the ions is converted into thermal energy of their random motion. The characteristic conversion time is $\tau \sim \omega^{-1}$ ($\omega = (4\pi ne^2/m)^{1/2}$ is the frequency of Langmuir oscillations (the plasma frequency)). Since the beam density is always changing, the phase advance of the plasma oscillations is estimated from the equation

$$\Delta\varphi = \int \omega(t)\, dt. \tag{9}$$

As long as $\Delta\varphi \ll 1$, we can assume that the positions of the ions have hardly changed, and mixing has not occurred. Mixing begins when $\Delta\varphi \sim 1$. Calculating the integral (9), we find

$$\Delta\varphi = \left(\frac{2m}{e}\right)^{1/4} \frac{J^{1/2}}{\alpha U^{3/4}} \ln \frac{r_2}{r_1}.$$

Here α is the aperture angle; r_1 and r_2 are the distances from the source between which the phase advance is calculated. For the electron beam considered below, J = 1 μA, U = 20 kV, $\alpha = 3\cdot10^{-3}$ rad, and $\Delta\varphi = 0.034 \ln (r_2/r_1)$. Mixing begins at $r_2/r_1 = \exp(0.034^{-1}) = 6\cdot10^{12}$, i.e., the mixing effect due to mutual repulsion can definitely be ignored. Similar results are obtained in the other examples that we are considering.

If two ions turn out to be very close together (at a distance $\ell \ll n^{-1/3}$), however, they will be strongly repelled and will separate rapidly, as a result of which the force acting on them decreases. The result is that the "tails" of the ion distribution function with respect to transverse velocities decay considerably faster than for the function $H(\beta_\perp)$ [$H(\beta_\perp) \sim \beta_\perp^{-5/2}$ as $\beta_\perp \to \infty$].

Second, mixing of ions can occur due to their different longitudinal velocities caused by the finite energy spread. It is simple to show that for a small velocity difference, the

mutual shift $\Delta\ell$ between two ions passing by at a distance r has the form $\Delta\ell = \Delta W/2W$ (ΔW is the energy spread). Mixing begins when the mutual shift assumes the same order as the mean distance between ions, i.e., $\Delta\ell \sim n^{-1/3}$. Estimates made for different cases show that this effect can also be ignored, as a rule.

And finally, mixing can occur due to nonisotropic expansion of the ion beam. We choose a coordinate system moving together with the ion beam, at the center of which lies some "test" ion, while the z axis is directed along the beam axis (Fig. 5). If the ion cloud expands isotropically, then the velocity of the i-th "field" ion in this coordinate system is

$$\mathbf{v}_i = A\mathbf{R}_i, \tag{10}$$

where A is a constant; $\mathbf{R}_i$ is the radius vector of the i-th ion (this situation is similar to the expansion of the universe, with A being analogous to the Hubble constant). In such an expansion the normalized field β at each point does not vary either in magnitude or in direction; only the normalization factor F^* decreases. The solution (8) was obtained for just this case. The beam expands only in the transverse direction, while the distance between ions does not change along the z axis.

We shall assume that the density decreases only due to isotropic expansion (10), onto which is superposed the motion

$$u_{zi} = -Az_i,\ u_{\rho i} = A\rho_i/2. \tag{11}$$

Here z_i and ρ_i are the coordinates of the i-th "field" ion in the cylindrical coordinate system, with the constants in (11) being chosen so that the anisotropic motion does not change the average density of the beam. The total velocity of the i-th ion is

$$\mathbf{V}_i = \mathbf{v}_i + \mathbf{u}_i,\ V_{zi} = 0,\ V_{\rho i} = \frac{3}{2}A\rho_i, \tag{12}$$

i.e., the total motion (12) correctly describes expansion of the beam in the moving coordinate system.

Let us estimate the rate of change of the transverse electric field $\mathbf{F}_\perp$ at the location of the "test" ion due only to the anisotropic motion (11) (the vector $\mathbf{F}_\perp$ lies in the plane perpendicular to the z axis). Since a given $\mathbf{F}_\perp$ field can be produced by different configurations of "field" ions, its rate of change $\mathbf{f}_\perp = d\mathbf{F}_\perp/dt$ can also be different. We shall not seek the probability distribution function $p(\mathbf{F}_\perp, \mathbf{f}_\perp)$ which determines the probability that the field $\mathbf{F}_\perp$ changes at the rate $\mathbf{f}_\perp$, but shall find the characteristic rate of change of the field $\mathbf{F}_\perp$. It is obvious that $\mathbf{F}_\perp = e\sum\frac{\boldsymbol{\rho}_i}{R_i^3}$, where $\boldsymbol{\rho}_i$ is a vector in the plane perpendicular to the z axis (see Fig. 5), and the sum is taken over all "field" ions. We then have

$$\mathbf{f}_\perp = e\sum\left(\frac{1}{R_i^3}\frac{\partial\boldsymbol{\rho}_i}{\partial t} - 3\frac{\boldsymbol{\rho}_i}{R_i^4}\frac{\partial R_i}{\partial t}\right). \tag{13}$$

Since we are considering only anisotropic motion (11), we have

$$\frac{\partial\boldsymbol{\rho}_i}{\partial t} = \frac{A}{2}\boldsymbol{\rho}_i,\ \frac{\partial R_i}{\partial t} = u_{\rho i}\sin\theta_i + u_{zi}\cos\theta_i = A\left(\frac{\rho_i}{2}\sin\theta_i - z_i\cos\theta_i\right)$$

and we can rewrite (13) as

$$\mathbf{f}_\perp = eA\sum\left(\frac{1}{2}\frac{\boldsymbol{\rho}_i}{R_i^3} - \frac{3}{2}\frac{\boldsymbol{\rho}_i}{R_i^3}\frac{\rho_i}{R_i}\sin\theta_i + 3\frac{\boldsymbol{\rho}_i}{R_i^3}\frac{z_i}{R_i}\cos\theta_i\right)$$

or

$$\mathbf{f}_\perp = eA\sum\frac{\boldsymbol{\rho}_i}{R_i^3}\left(\frac{1}{2} - \frac{3}{2}\sin^2\theta_i + 3\cos^2\theta_i\right). \tag{14}$$

Substituting into (14) the values of $\sin^2$ and $\cos^2$ averaged over the solid angle, we have

$$\mathbf{f}_\perp = \frac{A}{2} e \sum \frac{\boldsymbol{\rho}_i}{R_i^3} = \frac{A}{2} \mathbf{F}_\perp. \tag{15}$$

Equation (15) does not pretend to be highly accurate, of course, but gives some typical value of $\mathbf{f}_\perp$.

The average lifetime τ of an ion configuration with a field strength $\mathbf{F}_\perp$ can be estimated to be $\tau = F_\perp/f_\perp = 2/A$. In this time a "field" ion that had the coordinate ρ_1 moves away to a distance

$$\rho_2 = \rho_1 + V_\rho \tau = \rho_1 + \frac{3}{2} A \rho_1 \tau = 4\rho_1,$$

i.e., the beam becomes fully mixed, having expanded fourfold. This mixing obviously cannot be neglected.

To allow for the mixing, let us imagine a situation in which the path traveled by the beam is divided into segments $[r_n; r_{n+1}]$, in each of which the normalized field $\beta_\perp$ acting on the "test" ion is the same, while it changes randomly upon the transition to another section. The increase in virtual size is then

$$a = \sqrt{\sum a_n^2} \tag{16}$$

[a_n is the increase in virtual size in the n-th section, calculated from Eq. (8)].

Let us find the sum (16) for the case in which each segment is ξ times larger than the next segment, i.e., $|r_n - r_{n+1}|/|r_{n+1} - r_{n+2}| = \xi$ ($\xi = 4$). We choose the first segment to be from r_{max} to r_{max}/ξ, the second from r_{max}/ξ to r_{max}/ξ^2, etc. From (8) and (16) we then find

$$a^2 = \left(a_0 - \frac{a_0}{\xi^{2/3}}\right)^2 + \left(\frac{a_0}{\xi^{2/3}} - \frac{a_0}{\xi^{4/3}}\right)^2 + \dots$$

or

$$a^2 = a_0^2 \left[\left(1 - \xi^{-2/3}\right)^2 + \frac{(1 - \xi^{-2/3})^2}{\xi^{4/3}} + \frac{(1 - \xi^{-2/3})^2}{(\xi^{4/3})^2} + \dots \right]. \tag{17}$$

Summing the progression (17), we obtain

$$a/a_0 = (1 - \xi^{-2/3})/\sqrt{1 - \xi^{-4/3}}. \tag{18}$$

Some values of the function (18) are given in Table 1. Allowance for the anisotropy of beam expansion thus leads to a slower increase in virtual size, i.e., the result calculated from Eq. (8) must be multiplied by the coefficient 0.66.

Let us now estimate the transverse electric field $F_\perp$ in the "individual" mode: $F_\perp(r) \sim \frac{e}{l_\parallel^2} \frac{D}{l_\parallel}$. If we consider two beams with the same angular intensity, but one of which is narrow (the individual mode) and the other broad (the charged cloud mode), then the ratio of the transverse fluctuation fields in these beams at the same distance r from the emitter is $F_\perp(r)/F^*(r) \sim (r/r^*)^{7/3}$. Here r^* is the distance at which the narrow beam changes from the "individual" mode to the charged cloud mode: $r^* = \ell_\parallel/2\alpha$.

Thus, in the "individual" mode, in which the inequality (5) is satisfied, transverse fluctuating fields in the beam decrease sharply, which suppresses the increase in the virtual size of the source.

TABLE 1

ξ	a/a_0	ξ	a/a_0	ξ	a/a_0
1,1	0,18	3	0,59	5	0,70
2	0,48	4	0,66	6	0,73
				10	0,80

COMPARISON WITH EXPERIMENT

As follows from (8), the main increase in virtual size occurs not near the source but at a large distance from it, i.e., the final virtual size depends essentially on the construction of the given ion- (or electron-) optical column. Let us consider three examples. In [4] the increase in the virtual size of an autoelectron emitter was calculated numerically by the Monte-Carlo method and it was measured experimentally. The virtual size of an EGD ion emitter was measured in [10], and a design for an ion-optical column for an ion source with field ionization was suggested in [11, 12].

Autoelectron Emitter. A one-lens column with a total length 21.5 cm, magnification M = 2.5, aperture angle at the target $\alpha = 3 \cdot 10^{-3}$ rad, and electron energy eU = 20 keV was used in [4]. Since the mutual arrangement of electrons in the beam before and after the lens was the same, the total virtual size is obtained as the sum of the virtual sizes before and after the lens, rather than the square root of the sum of their squares. In Fig. 6 we give data from [4] for the beam diameter at the target (points: experiment; solid curve: calculation by the Monte-Carlo method) and the results of calculations from Eqs. (8) and (18). Since it was not indicated in [4] at what height the beam diameter was measured, the calculations were made for the diameter at half-height, $a_{0.5}$, and for the diameter at 1/10 of the maximum height $a_{0.1}$ (dashed lines 2 and 1, respectively). At high currents the calculated results agree fairly well with experiment; at low currents the beam diameter is determined by other factors (probably by chromatic aberration), and the contribution of the virtual size is negligible.

EGD Ion Source. The virtual size of an EGD source was measured in [10] in a column whose construction was described in [13]. In that column a beam of gallium ions is accelerated to an energy eU = 50 keV and with an angular intensity $I = 75$ μA/rad² it travels a distance $r \approx 7.5$ cm to the aperture diaphragm. The virtual size increases in this section, since after the diaphragm the beam moves in the "individual" mode. The calculated value of the virtual size of the source in such a column, $a_{0.5} = 22$ nm, agrees fairly well with the experimental value, 40 ± 20 nm [10]. Such calculations were also made in [8]. The brightness of the EGD source was also measured in [14], but there the brightness was found to be an order of magnitude lower than in [10], probably because of aberration on the grids used in [14].

Ion Source with Field Ionization. The virtual sizes of ion sources with field ionization have not been measured; it is only noted that they should be very small [15]. The construction of a source with field ionization was described in [11], and a design of an ion-optical column for it was suggested in [12]. To calculate the virtual size of the source we used the diagram of the ion-optical column (Fig. 7) copied from [11, 12].

The ion energy in the column is 50 keV, with the beam being accelerated in the first 20 mm section from the needle 1 to the accelerating lens 2. The angular intensity in the first section is $I = 15$ μA/rad²; for the beam current after the aperture diaphragm 3 we took two extreme values: $J_{min} = 2 \cdot 10^{-10}$ A and $J_{max} = 5 \cdot 10^{-9}$ A. For a total source current $J_0 = 10^{-8}$ A the ions will travel from the needle to the aperture diaphragm in the charged cloud mode. After the aperture diaphragm the picture changes. At the crossover, where the beam is narrow, the ions travel in the individual mode, and far from the crossover they travel in the charged cloud mode. In the sections of 85, 65, and 210 mm up to the second lens 4, $I = 840$ μA/rad², and simple calculations show that at a beam current J_{min} the change in mode occurs at a distance $r^* = 320$ cm from the crossover, while at J_{max} it occurs at $r^* = 2.6$ cm. We can thus assume that at J_{min} the growth in virtual size occurs only up to the aperture diaphragm, while at J_{max} it occurs over almost the entire length of the column. Assuming a point source and an absence of any aberrations, with allowance for the magnification of the optical system it is simple to obtain the size of the focused beam at the target 5: $d = 28$ nm at J_{min} =

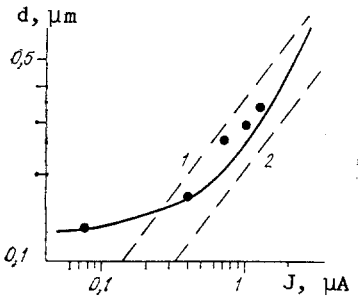

Fig. 6

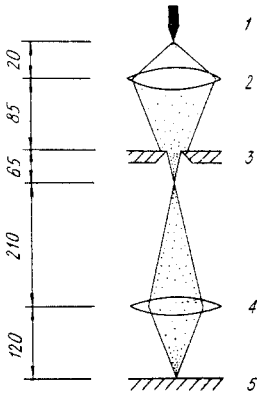

Fig. 7

$2 \cdot 10^{-10}$ A and d = 96 nm at $J_{max} = 5 \cdot 10^{-9}$ A, i.e., due only to the increase in the virtual size of the source, the current density in the focused beam cannot exceed 32 A/cm^2 in the first case and 69 A/cm^2 in the second, instead of the expected value of several hundred amperes per square centimeter [12]. The situation is not as bad as it seems at first glance, however.

First, our calculations may turn out to be inaccurate, since the required parameters of the ion-optical column must be determined from the available indirect data on it. Second, ways of suppressing the increase in virtual size are seen. For this one must choose a beam current such that the ions travel in the individual mode everywhere after the aperture diaphragm, and the aperture diaphragm must be placed closer to the source. To reduce the influence of the initial section, in which the charged cloud mode occurs, the magnification of the optical system should be as small as possible.

The effect of the increase in the virtual size of the emitter due to Coulomb repulsion between randomly distributed ions thus plays an important role in forming beams from very bright quasi-point sources. For autoelectron and EGD emitters the calculated results agree well with experiment, while for gas sources with field ionization, a considerable increase in virtual size in the process of acceleration and transport is predicted. The situation is not catastrophic, however, and with the proper design of ion-optical columns with allowance for this effect, the increase in virtual size can be suppressed to a considerable extent.

The author wishes to thank Professor V. G. Dudnikov for discussions and valuable comments.

APPENDIX

The procedure for measuring virtual size has been described in greatest detail in [10], in which lines at different linear doses were exposed in a resist. The virtual size of the source was determined from the ratio of their widths. The probability distribution function of the electric field component $\beta_\perp$ along the axis perpendicular to the beam and to the scanning direction (the so-called one-dimensional Holtsmark distribution) is obviously of interest in this case. Choosing the z axis to be along this component, we have $\beta_\perp = \beta \cos\theta$. The probability of appearance of the field $\beta_\perp$ is

$$dW(\beta_\perp) = H(\beta)\, d\beta \frac{2\pi \sin\theta\, d\theta}{4\pi}.$$

Substituting $\sin\theta\, d\theta = d\beta_\perp/\beta$ and integrating, we obtain

$$dW(\beta_\perp) = \frac{d\beta_\perp}{2} \int_{\beta_\perp}^{\infty} \frac{H(\beta)}{\beta} d\beta.$$

The current density distribution in the focal spot is determined by the probability distribution function of the field component β_ρ, lying in the plane perpendicular to the beam axis (the so-called two-dimensional Holtsmark distribution). Choosing the z axis to be along the beam, we have $\beta_\rho = \beta \sin\theta$. The probability of appearance of the field β_ρ is

$$dW(\beta_\rho) = H(\beta)\, d\beta \frac{2\pi \sin\theta\, d\theta}{4\pi}.$$

Substituting $d\theta = d\beta_\rho/(\beta \cos\theta)$ and integrating, we find

$$dW(\beta_\rho) = \frac{1}{2}\beta_\rho\, d\beta_\rho \int_{\beta_\rho}^{\infty} \frac{H(\beta)\, d\beta}{\beta\sqrt{\beta^2 - \beta_\rho^2}}.$$

The ρ coordinate of an ion in the plane of the spot is proportional to β_ρ, and the current density distribution is $j(\beta_\rho) \sim dW(\beta_\rho)/(2\pi\beta_\rho d\beta_\rho)$.

The function $H(\beta_\perp)$ has a full width at half-height of just under 3, and $j(\beta_\rho)$ is about 2.8. Either of them can therefore be used to calculate the virtual size $a_{0.5}$. These functions have considerably different asymptotic behavior, however. Since the three-dimensional Holtsmark distribution is $H(\beta) \sim \beta^{-5/2}$ for large β (this is easy to show, assuming that the high field strengths are produced by one nearby ion), we have $H(\beta_\perp) \sim \beta_\perp^{-5/2}$ and $j(\beta_\rho) \sim \beta_\rho^{-7/2}$.

Tables and graphs of one-, two-, and three-dimensional Holtsmark distributions can be found in [16], where more convenient equations for calculating those functions are also given.

LITERATURE CITED

1. G. I. Budker and A. N. Skrinskii, "Electronic cooling and new possibilities in the physics of elementary particles," Usp. Fiz. Nauk, 124, No. 4 (1978).
2. S. van der Meer, "Stochastic cooling and storage of antiprotons," Usp. Fiz. Nauk, 147, No. 2 (1985).
3. A. L. Shabalin, "Size of the emission zone of an electrohydrodynamic ion emitter," Dokl. Akad. Nauk SSSR, 303, No. 2 (1988).
4. T. Groves, D. L. Hammond, and H. Kuo, "Electron-beam broadening effects caused by discreteness of space charge," J. Vac. Sci. Technol., 16, No. 6 (1979).
5. J. W. Ward, "A Monte-Carlo calculation of the virtual source size for an LMIS," J. Vac. Sci. Technol., B3, No. 1 (1985).
6. W. Knauer, "Energy broadening in field emitted electron and ion beams," Optik, 56, No. 4 (1981).
7. G. H. Jansen, "Coulomb interaction in particle beams," Nucl. Instrum. Methods, A298, Nos. 1-3 (1990).
8. V. G. Dudnikov and A. L. Shabalin, "Evolution of the momentum distribution of ions in electrohydrodynamic ion emitters," Zh. Tekh. Fiz., 60, No. 4 (1990).
9. S. Chandrasekhar, Rev. Mod. Phys., 15, No. 1 (1943).
10. M. Kamuro, T. Kanayama, H. Hiroshima, and H. Tanoue, "Measurement of virtual crossover in liquid gallium ion sources," Appl. Phys. Lett., 42, No. 10 (1983).
11. G. N. Lewis, H. Paik, J. Mioduszewski, and B. M. Siegel, "A hydrogen field ion source with focusing optics," J. Vac. Sci. Technol., B4, No. 1 (1986).
12. G. N. Lewis, J. Mioduszewski, D. Weiner, and B. M. Siegel, "An ion beam lithography system for nanolithography with a focused H_2^+ ion probe," J. Vac. Sci. Technol., B6, No. 1 (1988).
13. M. Kamuro, "Ion beam exposure apparatus using a liquid metal source," Thin Solid Films, 92, Nos. 1-2 (1982).
14. G. D. Alton and P. M. Read, "Emittance measurements of gallium liquid-metal ion sources," Nucl. Instrum. Methods, B54, Nos. 1-3 (1991).
15. R. J. Blackwell, J. A. Kubby, G. N. Lewis, and B. M. Siegel, "Experimental focused ion beam system using a gaseous field ion source," J. Vac. Sci. Technol., B3, No. 1 (1985).
16. J. W. Ward, R. L. Kubena, and M. W. Utlaut, "Transverse thermal velocity broadening of focused beams from liquid ion sources," J. Vac. Sci. Technol., B6, No. 6 (1988).